European **J**ournal of **Chem**istry

Study of expired Fuclo 500 drug as an environmentally sustainable corrosion inhibitor

Aphouet Aurélie Koffi [iD] [1], N'guadi Blaise Allou [iD] [1,*], Mougo André Tigori [iD] [2],
Teminfolo Yaya Soro [iD] [1], Albert Trokourey [iD] [1] and Paulin Marius Niamien [iD] [1]

[1] *Laboratoire de Constitution et Réaction de la Matière, Unité de Formation et de Recherche des Sciences des Structures de la Matière et de Technologie, Université Félix Houphouët Boigny, Abidjan, Côte d'Ivoire*
[2] *Laboratoire des Sciences et Technologies de l'Environnement, Unité de Formation et de Recherche Environnement, Université Jean Lorougnon Guédé, Daloa, Côte d'Ivoire*

* *Corresponding author at: Laboratoire de Constitution et Réaction de la Matière, Unité de Formation et de Recherche des Sciences des Structures de la Matière et de Technologie, Université Félix Houphouët Boigny, Abidjan, Côte d'Ivoire.*
 e-mail: alloub.neist15a@acsir.res.in (N.B. Allou).

RESEARCH ARTICLE

ABSTRACT

This work deals with aluminium corrosion inhibition by expired drugs containing flucloxacillin in 1 M hydrochloric acid medium, using the gravimetric method and density functional theory. Weight loss results showed that the inhibitory efficiency of this compound increases with concentration and decreases with increasing temperature. The study also indicates that this molecule is adsorbed according to the modified Langmuir model (Villamil model). Furthermore, the thermodynamic parameters of adsorption (ΔG^o_{ads}, ΔH^o_{ads}, ΔS^o_{ads}) and activation (E_a^*, ΔH_a^*, ΔS_a^*) show that the adsorption is mixed type (chemisorption and physisorption). In addition, density functional theory provides access to the quantum chemical parameters of the molecule such as the lowest vacant orbital energy (E_{LUMO}), the highest occupied orbital energy (E_{HOMO}), the absolute electronegativity (χ), the global hardness (η), the global softness (S), the fraction of transferred electrons (ΔN) as well as the electrophilicity index (ω) for finding correlation between the inhibitor structure and the experimental data.

1. Introduction

Metallic materials and more particularly aluminium are corrosion sites in an acid environment. The use of corrosion inhibitors is the most suitable and economical method to cope with this phenomenon that generates several problems [1-3]. However, fighting against corrosion without taking into account environmental pollution is another more serious one. In fact, the directives on industrial waste are becoming increasingly stringent. Therefore, environmental protection has become an essential issue for every nation in the last decade. Developing biodegradable and eco-compatible corrosion inhibitors is now a major challenge [4-6].

Current studies are directed towards the development of organic compounds that are non-toxic and stable at high temperatures [4], leading several researchers to take an interest in pharmaceutical products. Therefore, several classes of molecules, including antibiotics [7,8], antifungals [9,10], analgesics [11], and vitamins [12,13], were used as corrosion inhibitors for metals in an acidic environment. In this light, the flucloxacillin

molecule has already shown inhibiting properties with respect to the corrosion of mild steel in sulfuric acid medium, but the inhibition mechanism was not clearly elucidated [14].

These organic inhibitors act by adsorption on the surface of the metal to be protected [15,16]. This action mechanism can be described using the thermodynamic adsorption and activation parameters of the inhibiting species. Quantum chemical calculations are very useful for investigating descriptor parameters and for better understanding the inhibition mechanism of molecules [17,18].

In this sense, this research project aims to investigate the inhibitory properties of expired Fuclo 500 tablets containing a flucloxacillin molecule in 1 M hydrochloric acid medium using the weight loss technique and DFT calculations. The study drug is six months out of date. In fact, expired drugs should be destroyed after their expiration date, and reuse as corrosion inhibitors for metals could have great economic value. Therefore, a large amount of money used for metal and alloy protection can be saved.
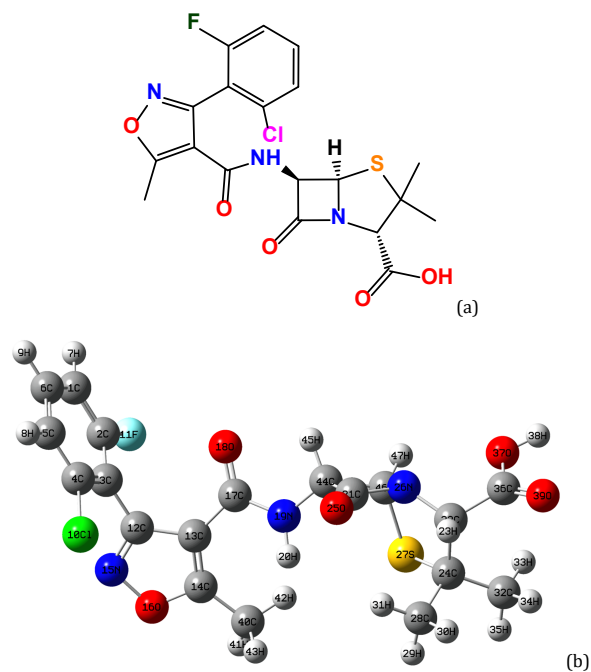
Figure 1. (a) Chemical structure and (b) optimised flucloxacillin structure by DFT/B3LYP/6-31G(d).

2. Experimental

2.1. Aluminium samples

An aluminium rod of 3 mm in diameter and 99.6% in purity is cut into 1 cm high. These samples are pre-treated to remove any impurity. This pre-treatment consisted of polishing them with abrasive paper, washing with acetone solution then with distilled water; finally, drying them in an oven at 343 K for 10 minutes.

2.2. Inhibitor

The molecule studied is flucloxacillin (Figure 1) with chemical formula $C_{19}H_{17}FClN_3O_5S$ and molar mass Mw = 453.87 g/mol contained in expired Fuclo 500 tablets.

2.3. Electrolyte medium

The aluminium samples were immersed in a 1 M hydrochloric acid solution without or with flucloxacillin. Inhibitor concentrations vary between 5×10^{-5} and 5×10^{-4} M.

2.4. Experimental method: Gravimetry

The corrosion rate and inhibition efficiency of the inhibitor tested were analysed at various temperatures (303-323 K) by determining the mass loss that the metal underwent after 1 hour of immersion in the electrolyte medium. The corrosion rate W (g.cm^{-2}.h^{-1}) is evaluated by the Equation (1):

$$W = \frac{\Delta m}{S.t} \tag{1}$$

where $\Delta m = m_1 - m_2$ is the mass loss (g); S is the total area of the specimen (cm^2) and t is the immersion time (h). The inhibition efficiency $E(\%)$ is calculated according to the expression below:

$$E(\%) = \frac{W_o - W}{W_o} \times 100 \tag{2}$$

where, W_o and W are the corrosion rates without and with inhibitor, respectively. The corrosion rate value is the average of three tests performed under the same conditions. The gravimetry results are comparable to those of other methods (electrochemical, thermometric, spectroscopic methods, *etc.*) used for the study of corrosion [19].

2.5. Theoretical analysis by density functional theory calculation

Quantum chemistry calculations were carried out to investigate the electronic properties of the molecule. In this study, the flucloxacillin molecule was drawn and preoptimized using GaussView 5. Calculations were performed using the Gaussian 09W software package [20] at DFT/B3LYP method [21,22] with 6-31G(d) basis set [23]. Global reactivity descriptors such as chemical potential (μ), hardness (η), softness (S), electronegativity (χ), and electrophilicity index (ω) were evaluated from the energy values of the highest occupied molecular orbital (HOMO) and the lowest unoccupied molecular orbital (LUMO).

3. Results and discussion

3.1. Aluminium corrosion rate and inhibitory efficiency of flucloxacillin

The corrosion rate of aluminium in 1 M hydrochloric acid medium was evaluated within a temperature range of 303 to 323 K. The results obtained are shown in Figure 2. It was observed that the metal dissolution rate in the corrosive medium is 0.0163 g.cm^{-2}h^{-1} at room temperature and increases up to 0.0755 g.cm^{-2}h^{-1} at T = 323 K. However, the addition of flucloxacillin to the acid medium reduces the corrosion rate. This decrease indicates that the corrosion inhibiting effect of the study molecule is improved by increasing the inhibitor concentration.

Therefore, the inhibition performance of flucloxacillin was plotted against the concentration of inhibitory species and the medium temperature (Figure 3).
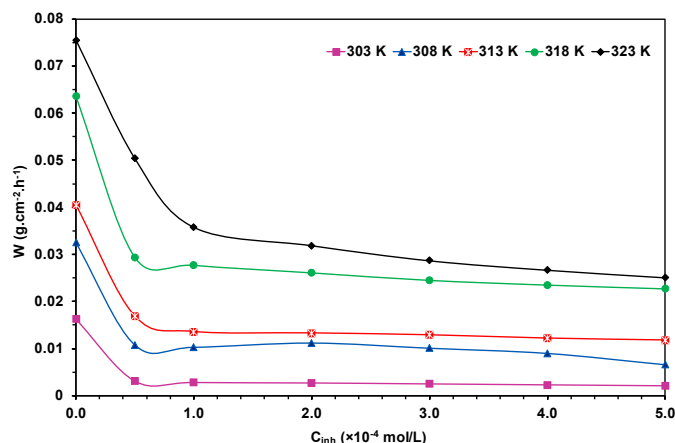
Figure 2. Evolution of the aluminium corrosion rate in 1 M HCl solution with flucloxacillin concentration at various temperatures.
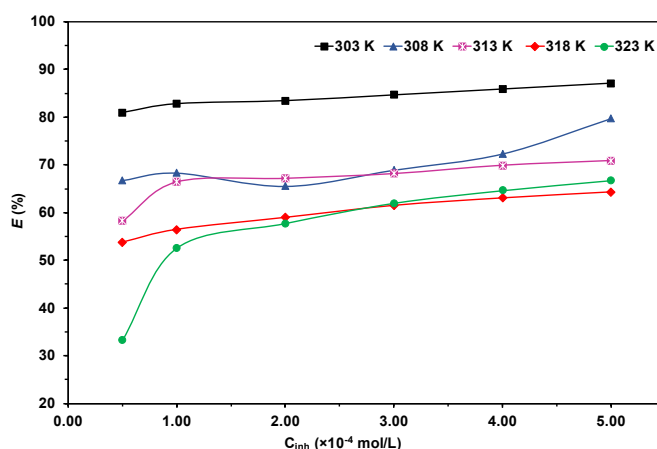

Figure 3. Plot of the evolution of inhibitory efficacy versus flucloxacillin concentration and temperature.

The figure shows that the inhibitory efficiency increases with the concentration of the inhibitor but decreases when the temperature increases. In fact, increasing temperature promotes the desorption of some inhibitory species from the metal surface, as well as the dissolution of the inhibiting barrier due to thermal agitation [24]. Therefore, the inhibition rate moved from 87.12 to 66.75% at room temperature and 323 K, respectively, with 5×10⁻⁴ M inhibitory species. However, this result is quite high compared to those found in the literature [25-27].

3.2. Adsorption isotherms

Adsorption isotherms are essential to understand the mechanism of the corrosion inhibition reaction [28]. Thus, to learn more about the adsorption process of flucloxacillin, the experimental data were correlated with some mathematical models, such as Langmuir and Dubinin-Radushkevich isotherms. The Langmuir adsorption isotherm describes the variation of C_{inh}/θ with C_{inh}. The experimental data gave straight lines (Figure 4a) with the best fit (Table 1) of this model.

Therefore, the Langmuir adsorption model explains the adsorption of flucloxacillin on the aluminium surface. However, the slopes of the obtained lines are higher than unity. This deviation from the ideal could be attributed to interactions between adsorbed species and the binding of an inhibitor to multiple adsorption sites [29]. To take the deviation into account, the corrected Langmuir model (Villamil model) with the following equation was considered:

$$\frac{C_{inh}}{\theta} = \frac{n}{K_{ads}} + nC_{inh} \tag{3}$$

The slope (n) and the intercept ($\frac{n}{K_{ads}}$) were used to calculate the adsorption equilibrium constant K_{ads}. In turn, K_{ads} values were used to determine the thermodynamic parameters.

In order to clarify the type of adsorption (chemisorption or physisorption) involved, the Dubinin-Radushkevich isotherm was also used in this study [27,30]. This model is described by Equation (4).

$$\ln\theta = ln\theta_{max} - a\delta^2 \tag{4}$$

In this expression, δ corresponds to the Polanyi potential and is defined as follows:

$$\delta = RT\ ln\ (1 + \frac{1}{C_{inh}}) \tag{5}$$

In addition, the constant a was used to calculate the average adsorption energy E_m (Equation (6)), corresponding to the energy required to move one mole of the adsorbate from infinity (solution) to the metal surface.

$$E_m = \frac{1}{\sqrt{2\ a}} \tag{6}$$

The plots of $ln\ \theta$ versus δ^2 are shown in Figure 4b. The maximum surface coverage θ_{max}, the parameter a as well as the calculated values of E_m are recorded in Table 1.

Table 1. Adsorption isotherm parameters for aluminium in 1 M HCl medium.

Temperature (K)	Langmuir isotherm		Dubinin-Radushkevich isotherm			
	R^2	Slope	R^2	a (kJ^{-2} mol^2)	θ_{max}	E_m (kJ/mol)
303	0.9997	1.1407	0.8902	0.0009	1.144	23.57
308	0.9873	1.2595	0.3793	0.0015	1.334	18.26
313	0.9996	1.3865	0.9075	0.0022	1.354	15.08
318	0.9992	1.5182	0.9586	0.0021	1.514	15.43
323	0.9984	1.3625	0.9332	0.0077	1.243	8.06
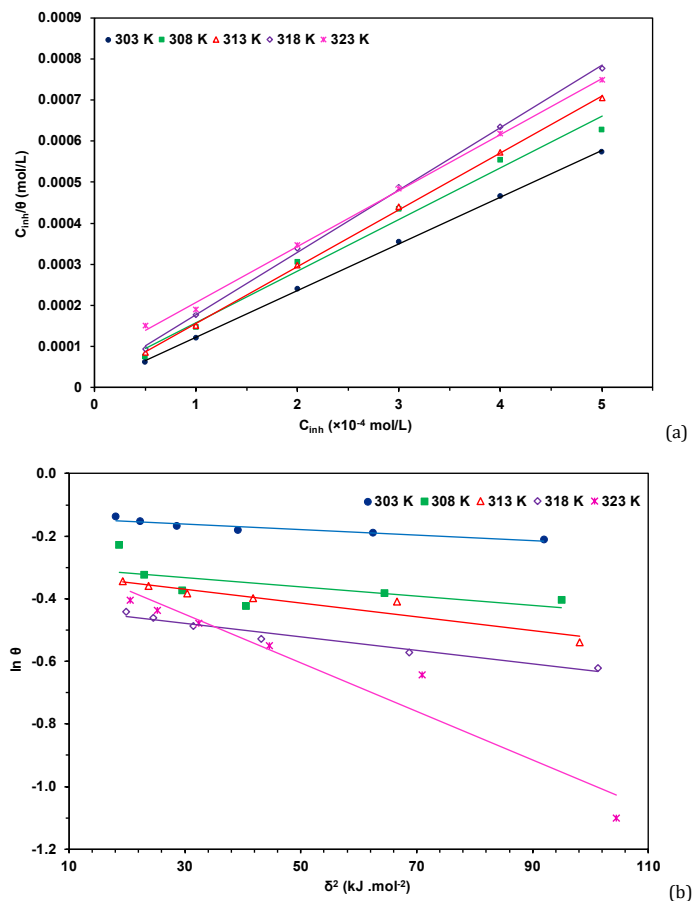
Figure 4. (a) Langmuir and (b) Dubinin-Radushkevich isotherms for the adsorption of flucloxacillin on aluminium in 1 M HCl medium at various temperatures.

According to Tan *et al.* [31], E_m values between 8 and 16 kJ/mol indicate that chemisorption is predominant, while values below 8 kJ/mol correspond to the physisorption of inhibiting species. As shown in Table 1, the average adsorption energy indicates that chemical bonds are formed between the inhibitor and the aluminium surface in the temperature range studied.

3.3. Thermodynamic parameters

3.3.1. Adsorption parameters

Thermodynamic adsorption parameters further distinguish physisorption from chemisorption [32]. Thus, the Gibbs free energy of adsorption (ΔG_{ads}^o) can be deduced from Equation (7):

$$K_{ads} = \frac{1}{55.5} \exp\left(-\frac{\Delta G_{ads}^o}{RT}\right) \qquad (7)$$

In which, 55.5 (in mol/L) corresponds to the concentration of water [33], R the perfect gas constant and T the absolute temperature. The standard adsorption enthalpy and entropy (ΔH_{ads}^o and ΔS_{ads}^o) can be obtained by using the Equation (8);

$$\ln K_{ads} = \frac{-\Delta H_{ads}^o}{RT} + \frac{\Delta S_{ads}^o}{R} - \ln C_{H_2O} \qquad (8)$$

Figure 5 represents the plot of $\ln K_{ads}$ against 1000/T giving a straight line with slope $-\Delta H_{ads}^o/R$ and intercept $-\Delta S_{ads}^o/R - \ln 55.5$. The values obtained are given in Table 2. The strong adsorption capacity of flucloxacillin on the aluminium surface in 1 M HCl is revealed through the high values of K_{ads}. Indeed, the flucloxacillin structure contains nitrogen, sulfur and oxygen heteroatoms and π electrons allowing for better protection against corrosion [34,35]. However, increasing the temperature from 303 to 313 K causes the value of K_{ads} to decrease, leading to the weakness of the protective layer. Furthermore, an exception is observed at 308 K due to the results obtained for C_{inh} = 2×10^{-4} M (Figure 3). Indeed, the flucloxacillin efficiency is not as expected. Consequently, the R^2 value is not close enough to unity, but it is acceptable. Besides, the negative values of ΔG_{ads}^o highlight the spontaneous adsorption of inhibitory species on the aluminium surface. Moreover, it is reported that ΔG_{ads}^o values for physisorption are higher than –20 kJ/mol while those of chemisorption are less than –40 kJ/mol [36]. In this study, the inhibitor shows mixed adsorption behaviour with a predominance of chemical adsorption.

Table 2. Thermodynamic adsorption parameters derived from the Langmuir isotherm for aluminium in 1M HCl with flucloxacillin.

T (K)	K_{ads} (L/mol)	$-\Delta G_{ads}^o$ (kJ/mol)	ΔH_{ads}^o (kJ/mol)	ΔS_{ads}^o (J/mol.K)
303	142588	40.00	−61.67	−73.39
308	41983	37.53		
313	69325	39.44		
318	50607	39.24		
323	19464	37.29		

Table 3. Thermodynamic parameters for aluminium dissolution in 1 M HCl without and with flucloxacillin.

C_{inh} (×10^{-4} mol/L)	E_a^* (kJ/mol)	ΔH_a^* (kJ/mol)	ΔS_a^* (J/mol.K)
0	61.000	58.399	309.683
0.5	107.348	104.750	449.842
1	99.425	96.825	423.240
2	94.599	92.000	407.566
3	94.352	91.753	406.150
4	95.923	93.324	410.552
5	101.324	98.723	426.934
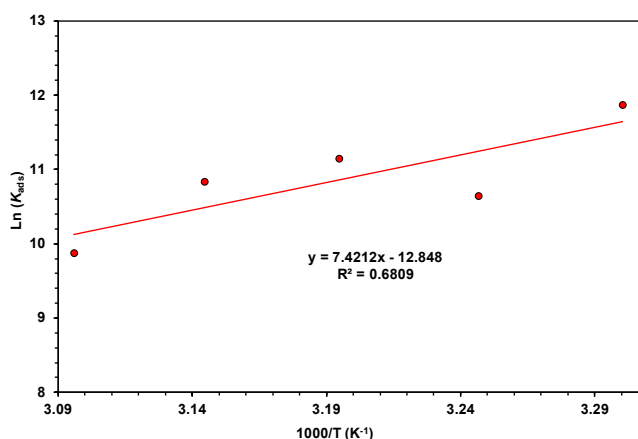
Figure 5. Plot of $ln\ K_{ads}$ versus 1000/T for aluminium in 1 M HCl with flucloxacillin.

Negative values of ΔS_{ads}^o confirm the adsorption of flucloxacillin. It also reflects a decrease in disorder during the adsorption of the inhibitor, since a compound in the condensed state is more ordered than in aqueous solution. The enthalpy variation ΔH_{ads}^o, accompanying this adsorption process is also negative, which indicates the exothermic nature of the phenomenon and is generally attributed to the presence of the two physisorption and chemisorption [35].

3.3.2. Activation parameters

To take into account the effect of temperature on the corrosion rate, the activation energy was determined using the Arrhenius equation (Equation (9)).

$$W = A \times exp\left(\frac{-E_a^*}{2.303 \times R \times T}\right) \tag{9}$$

The plot of $log\ W$ against 1000/T (Figure 6a) was used to determine the activation energy (Table 3). The data show that E_a^* is higher in the presence of inhibitor.

The increase of the concentration of flucloxacillin reveals that aluminium dissolution decreases as a result of the formation of an energy barrier by the adsorbed inhibitors on the substrate surface. The comparison of the values obtained also underlines the type of absorption [19,37,38]. According to the results, E_a^* is higher in the presence of inhibitor, so physical adsorption is responsible for the inhibitory properties of flucloxacillin. However, a decrease in E_a^* values can be observed as inhibitor amount increases. This decrease is attributed to a slight improvement with increasing flucloxacillin concentration. Thus, the corrosion rate does not decrease as much as expected by increasing C_{inh} (Figure 2). This slow decrease is

therefore reflected in the plot of $log\ W$ versus 1000/T because the points are almost the same at a given temperature. Enthalpy and entropy activation values for metal corrosion can be determined from the alternative formula of the Arrhenius equation given below:

$$W = \frac{R.T}{N.h} exp\left(\frac{\Delta S_a^*}{R}\right). exp\left(-\frac{\Delta H_a^*}{R.T}\right) \tag{10}$$

The plot of $log(\frac{W}{T})$ versus 1000/T gives Figure 6b. Values of enthalpy ΔH_a^* and entropy ΔS_a^* of activation are given in Table 3. The activation enthalpy is positive, reflecting the endothermic nature of the aluminium dissolution process without and with the addition of inhibitor [32]. Moreover, magnitude of ΔH_a^* almost matches with E_a^*, confirming the endothermic process of dissolution. Besides, activation entropy values are more positive in the presence of flucloxacillin, showing better resistance of aluminium in the aggressive solution and a dissociative mechanism during which the activated complex is loosely bound and about to dissociate [39]. Similarly, ΔH_a^* and ΔS_a^* values decrease when flucloxacillin is more concentrated. This behaviour is due to overlapping points.

3.4. Analysis of the electronic properties of flucloxacillin by DFT

3.4.1. Global reactivity descriptors

Theoretical quantum chemistry is a very useful tool for understanding the behaviour of species and particularly the corrosion inhibition mechanism. Therefore, several electronic parameters of flucloxacillin were studied using DFT.

Table 4. Quantum chemical parameters of neutral flucloxacillin by B3LYP/6-31G(d).

E_{HOMO} (eV)	E_{LUMO} (eV)	ΔE (eV)	μ (D)	E_T (Ha)	χ (eV)	η (eV)	S (eV^{-1})	ω (eV)	ΔN
−6.688	−1.012	5.676	4.431	−2232.817	3.850	2.838	0.352	2.611	0.076
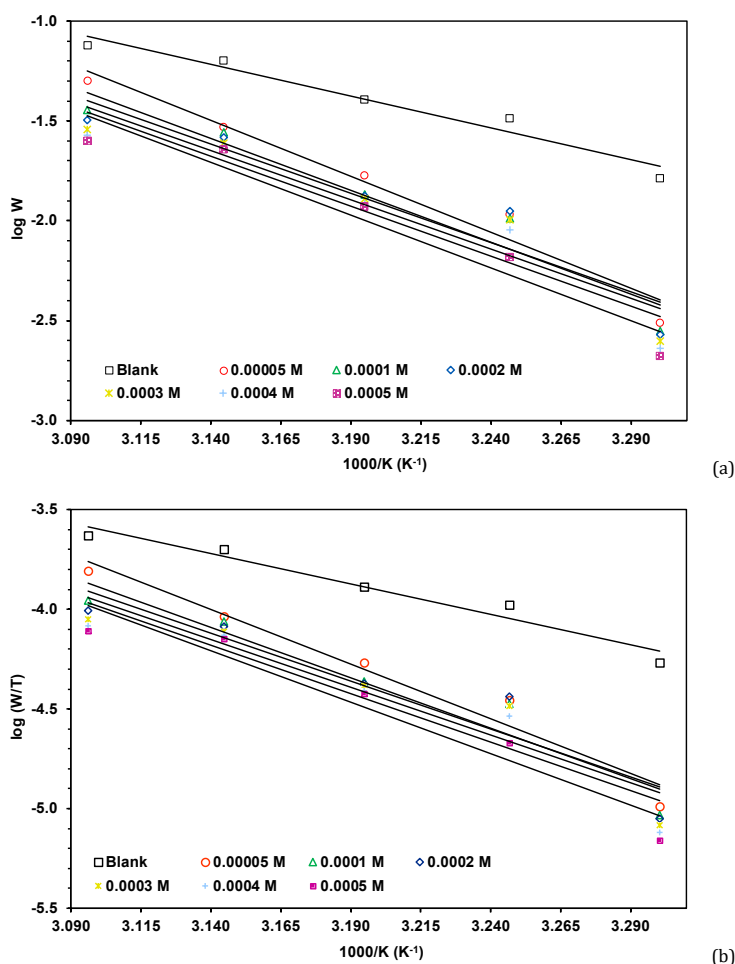
Figure 6. Plots of (a) *log W* and (b) *log (W/*T*)* versus 1000/T for aluminium immersed in 1 M HCl without and with flucloxacillin.

On the one hand, the optimised structure as well as the electronic densities of the highest occupied (HOMO) and lowest vacant (LUMO) molecular orbitals (Figure 7) were obtained. On the other hand, DFT was used to determine the descriptor parameters of the studied molecule, namely, energy of frontier molecular orbitals, energy gap, electrophilicity index, *etc*. The values of these various parameters are reported in Table 4.

Figure 7 shows that the HOMO density of the studied molecule is almost localised over the entire molecule, while the LUMO density is mainly distributed over the isoxazole ring. The ability for a chemical species to donate or receive electrons is associated with the frontier orbitals energies E_{HOMO} and E_{LUMO}, respectively. Thus, compared to the literature [21-23], E_{HOMO} is high and E_{LUMO} low. Accordingly, the inhibitory properties of flucloxacillin are due to its capacity to exchange electrons with the aluminium surface. Moreover, the chemical reactivity of an organic molecule is closely correlated with a low energy gap (ΔE) between LUMO and HOMO orbitals [4,24]. Therefore, the value of 5.676 eV corroborates interactions between the molecule and the substrate.

DFT calculations also provide for the molecule electronegativity χ, the electrophilicity index ω, the hardness η and the softness *S* parameters. The first parameter characterises the tendency of a chemical species to attract electrons toward itself. The second measures the propensity of a chemical species to accept electrons, while hardness and softness evaluate both stability and reactivity of a molecule [40,41]. In this study, the theoretical value of 3.850 eV is lower than 4.280 eV of the aluminium work function (ϕ_{Al} was rather used because χ_{Al} is conceptually wrong here). Therefore, during interactions, electrons flow from flucloxacillin to the aluminium surface with a fraction of transferred electrons $\Delta N = 0.076$ eV [35].

3.4.2. Local selectivity

The Fukui functions (f_k^+, f_k^-) and the dual descriptor Δf_k were calculated to analyse the selective reactivity of flucloxacillin molecule (Table 5). The first parameter can be obtained, for each atom of a species, from the following Equations:

$$f^+(\vec{r}) = q_k(N + 1) - q_k(N) \tag{11}$$

$$f^-(\vec{r}) = q_k(N) - q_k(N + 1) \tag{12}$$

$q_k(N), q_k(N - 1),$ and $q_k(N + 1)$ are Mulliken charge of k atom in the neutral, anionic and cationic system, respectively.

Table 5. Pertinent Mulliken charges, Fukui functions and dual descriptor of flucloxacillin by B3LYP/6-31G(d).

Atom no	$q_k(N+1)$	$q_k(N)$	$q_k(N-1)$	f_k^+	f_k^-	Δf_k
C1	−0.211	−0.200	−0.173	−0.011	−0.027	0.016
C2	0.324	0.400	0.390	−0.076	0.010	−0.086
C3	−0.020	0.025	0.063	−0.045	−0.038	−0.007
C4	−0.139	−0.094	−0.103	−0.045	0.009	−0.054
C5	−0.143	−0.141	−0.115	−0.002	-0.026	0.024
C6	−0.179	−0.117	−0.110	−0.062	−0.007	−0.055
Cl10	−0.078	0.008	0.123	−0.086	−0.115	0.029
F11	−0.311	−0.280	−0.264	−0.031	−0.016	−0.015
C12	0.188	0.223	0.236	−0.035	−0.013	−0.022
C13	−0.071	−0.094	−0.101	0.023	0.007	0.016
C14	0.393	0.386	0.408	0.007	−0.022	0.029
N15	−0.295	−0.207	−0.188	−0.088	−0.019	−0.069
O16	−0.407	−0.363	−0.342	−0.044	−0.021	−0.023
C17	0.513	0.589	0.588	−0.076	0.001	−0.077
O18	−0.544	−0.513	−0.491	−0.031	−0.022	−0.009
N19	−0.583	−0.625	−0.601	0.042	−0.024	0.066
C21	0.581	0.574	0.594	0.007	−0.020	0.027
C22	−0.005	−0.071	−0.093	0.066	0.022	0.044
C24	−0.091	−0.095	−0.134	0.004	0.039	−0.035
O25	−0.492	−0.461	−0.394	−0.031	−0.067	0.036
N26	−0.454	−0.409	−0.398	−0.045	−0.011	−0.034
S27	0.093	0.075	0.312	0.018	−0.237	0.255
C28	−0.440	−0.451	−0.457	0.011	0.006	0.005
C32	−0.472	−0.458	−0.470	−0.014	0.012	−0.026
C36	0.576	0.602	0.617	−0.026	−0.015	−0.011
O37	−0.580	−0.557	−0.567	−0.023	0.010	−0.033
O39	−0.456	−0.458	−0.425	0.002	−0.033	0.035
C40	−0.528	−0.558	−0.567	0.030	0.009	0.021
C44	−0.074	−0.060	−0.093	−0.014	0.033	−0.047
C46	−0.134	−0.129	−0.132	−0.005	0.003	−0.008
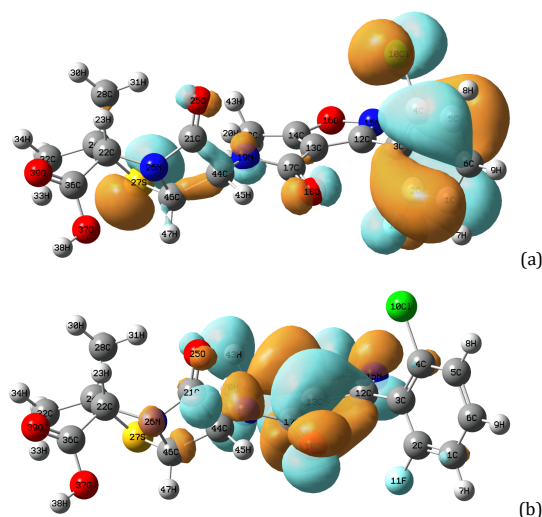
Figure 7. (a) HOMO and (b) LUMO maps of flucloxacillin using B3LYP/6-31G(d).

The dual descriptor Δf_k can be defined as the difference between $f^+(\vec{r})$ and $f^-(\vec{r})$, respectively the nucleophilic and electrophilic Fukui functions [42].

$$\Delta f_k = f_k^+ - f_k^- \qquad (13)$$

This parameter is positive in the electrophilic zones and negative in the nucleophilic zone [33]. Therefore, the most positive value of Δf_k indicate that the site may be favoured for attack by a nucleophile, whereas the site expected for electrophilic attack is indicated by the most negative value of Δf_k. Moreover, maximum values of f_k^+ and f_k^- are also important in determining the preferred sites for attack by nucleophile and electrophile, respectively.

In the molecule studied, N19 and C22 exhibit the highest values of the nucleophilic attack index (f_k^+). However, the highly positive dual descriptor (Δf_k) suggests that S27 may be a good electrophilic site. Otherwise, the nucleophilic attack site should belong to the HOMO of the molecule. Therefore, the probable zones for attack by a nucleophilic are N19 and S27.

Analysis of these results also shows that the highly negative values of Δf_k are localized on the atoms C2, C4, C6, C17 and N15 implying that these sites are electrons acceptors. The highest values of f_k^- suggest, on the contrary, that C24 and C44 act as nucleophilic zones. However, the LUMO map of the fluclo-xacillin molecule supports that the preferred sites for electrophilic attack are C2, C17, and N15.

3.5. Corrosion and inhibition mechanism

3.5.1. Corrosion process mechanism

The metal is naturally covered with a protective layer of aluminium oxide. However, this barrier film is damaged in acid medium and the metal dissolves according to the following equations:

$$Al \rightarrow Al^{3+} + 3e^- \qquad (14)$$

$$3H^+ + 3e^- \rightarrow \frac{3}{2}H_2 \qquad (15)$$

As a result, corrosion leads to complete dissolution of the metal or depletion of the H^+ protons in the electrolyte. This mechanism is generally not affected by the addition of an organic inhibitor that acts by adsorption on the metal surface [43].

3.5.2. Adsorbed species inhibition mechanism

Adsorption depends mainly on the substrate surface charge and the inhibitor structure. Thus, molecular and protonated flucloxacillin can participate in the inhibition of aluminium corrosion. In acidic medium, the inhibitor molecule can be protonated due to its heteroatom according to the following equation.

$$[Inh] + x\,H^+ \rightarrow [InhH_x]^{x+} \qquad (16)$$

Adsorption of the formed $[InhH_x]^{x+}$ would occur on the metal surface previously charged by the Cl^- ions. Indeed, the adsorption of chloride ions facilitates that of inhibiting cations [44]. In addition, these cations can be adsorbed in competition with H^+ ions [13]. Interactions between protonated inhibitors and the aluminium surface could be electrostatic in nature but could be also due give rise to chemical bonds [44].

Inhibition of aluminium corrosion can also be performed through the adsorption of metal complexes formed by the combination of Al^{3+} ions and flucloxacillin [45].

Besides these inhibitory cations, molecular flucloxacillin can replace previously adsorbed water molecules through the following relationship:

$$Inh_{(sol)} + n\,H_2O_{ads} \rightarrow Inh_{ads} + n\,H_2O_{(sol)} \qquad (17)$$
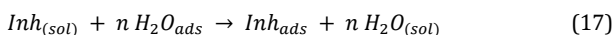
However, the steric hindrance of the inhibitory species would not facilitate its adsorption and would constitute an obstacle to greater inhibitory efficacy.

4. Conclusion

The study of the corrosion rate in the absence and presence of flucloxacillin at various concentrations and temperatures showed that the chosen molecule has inhibiting properties. Inhibition efficiency increases with flucloxacillin concentration but decreases with increasing temperature. The adsorption isotherms revealed that an inhibiting species adsorbs at several sites, and there are repulsions between adsorbed species, which characterises the Villamil (or modified Langmuir) model. Furthermore, thermodynamic adsorption parameters (ΔG^o_{ads}, ΔH^o_{ads} ΔS^o_{ads}) indicate that the adsorption of the inhibitor is mixed (physisorption and chemisorption) and is facilitated by the presence of heteroatoms. The descriptors of global reactivity indicate a possible protonation of the flucloxacillin molecule. DFT results also showed that HOMO is distributed throughout the molecule while LUMO is mainly localised around the isoxazole ring. The positive value of ΔN confirms the preponderance of chemisorption in the adsorption process between flucloxacillin and aluminium. Electronegativity χ also indicates that during interactions, electrons mainly flow from flucloxacillin to the aluminium surface. Thus, DFT corroborates the gravimetric findings because the inhibiting species can share electrons with other species in the medium.

Disclosure statement ⓓ

Conflict of interest: The authors declare that they have no conflict of interest.
Ethical approval: All ethical guidelines have been adhered to.
Sample availability: Samples of the compounds are available from the author.

CRediT authorship contribution statement ⓒⓡ

Conceptualization: Aphouet Aurélie Koffi; Methodology: Aphouet Aurélie Koffi; Software: Aphouet Aurélie Koffi; Formal Investigation: Aphouet Aurélie Koffi, Teminfolo Yaya Soro; Writing - Original Draft: Teminfolo Yaya Soro, Aphouet Aurélie Koffi; Writing - Review and Editing: N'guadi Blaise Allou; Supervision: Albert Trokourey, Paulin Marius Niamien.

ORCID ⓘⒹ and Email ✉

Aphouet Aurélie Koffi
✉ koffiaphouet@yahoo.fr
ⓘⒹ https://orcid.org/0000-0003-2306-7593
N'guadi Blaise Allou
✉ allounguadi@yahoo.fr
✉ alloub.neist15a@acsir.res.in
ⓘⒹ https://orcid.org/0000-0002-4367-2128
Mougo André Tigori
✉ tigori20@yahoo.fr
ⓘⒹ https://orcid.org/0000-0002-3722-7896
Teminfolo Yaya Soro
✉ teminfolosoro@gmail.com
ⓘⒹ https://orcid.org/0009-0001-1494-7452
Albert Trokourey
✉ trokourey@gmail.com
ⓘⒹ https://orcid.org/0000-0001-7139-5976
Paulin Marius Niamien
✉ niamienfr@yahoo.fr
ⓘⒹ https://orcid.org/0000-0002-0744-9623

References

[1]. *Functional materials: Preparation, processing and applications*; Banerjee, S.; Tyagi, A. K., Eds.; Elsevier Science Publishing: Philadelphia, PA, 2011.

[2]. Kutz, M. *Handbook of environmental degradation of materials*; 2nd ed.; William Andrew Publishing: Norwich, CT, 2012.

[3]. Plieth, W. *Electrochemistry for Materials Science*; Elsevier Science: London, England, 2007.

[4]. Herrag, L.; Hammouti, B.; Elkadiri, S.; Aouniti, A.; Jama, C.; Vezin, H.; Bentiss, F. Adsorption properties and inhibition of mild steel corrosion in hydrochloric solution by some newly synthesized diamine derivatives: Experimental and theoretical investigations. *Corros. Sci.* **2010**, *52*, 3042–3051.

[5]. Chevalier, M.; Robert, F.; Amusant, N.; Traisnel, M.; Roos, C.; Lebrini, M. Enhanced corrosion resistance of mild steel in 1M hydrochloric acid solution by alkaloids extract from Aniba rosaeodora plant: Electrochemical, phytochemical and XPS studies. *Electrochim. Acta* **2014**, *131*, 96–105.

[6]. Gece, G. Drugs: A review of promising novel corrosion inhibitors. *Corros. Sci.* **2011**, *53*, 3873–3898.

[7]. Eddy, N. O.; Odoemelam, S. A. Inhibition of the corrosion of mild steel in acidic medium by penicillin V potassium. *Advances in Natural and Applied Sciences* **2008**, *2*, 225-232 http://www.aensiweb.com/old/anas/2008/225-232.pdf.

[8]. Eddy, N. O.; Odoemelam, S. A.; Ekwumemgbo, P. Inhibition of the corrosion of mild steel in HSO by penicillin G. *Sci. Res. Essays* **2009**, *4*, 33-38 https://academicjournals.org/article/article1380720172_Eddy%20et%20al%20Pdf.pdf.

[9]. Obot, I. B. Synergistic effect of nizoral and iodide ions on the corrosion inhibition of mild steel in sulphuric acid solution. *Port. Electrochim. Acta* **2009**, *27*, 539–553.

[10]. Obot, I. B.; Obi-Egbedi, N. O. Inhibition of aluminium corrosion in hydrochloric acid using nizoral and the effect of iodide ion addition. *E-J. Chem.* **2010**, *7*, 837–843.

[11]. Prabhu, R. A.; Shanbhag, A. V.; Venkatesha, T. V. Influence of tramadol [2-[(dimethylamino)methyl]-1-(3-methoxyphenyl) cyclohexanol hydrate] on corrosion inhibition of mild steel in acidic media. *J. Appl. Electrochem.* **2007**, *37*, 491–497.

[12]. Kesari, P.; Udayabhanu, G. Investigation of Vitamin B12 as a corrosion inhibitor for mild steel in HCl solution through gravimetric and electrochemical studies. *Ain Shams Eng. J.* **2023**, *14*, 101920.

[13]. Solmaz, R. Investigation of corrosion inhibition mechanism and stability of Vitamin B1 on mild steel in 0.5M HCl solution. *Corros. Sci.* **2014**, *81*, 75–84.

[14]. Alfakeer, M.; Chemistry Department, Faculty of Science, Princess Nourah bint Abdulrahman University, Riyadh, Saudi Arabia Corrosion inhibition effect of expired ampicillin and flucloxacillin drugs for mild steel in aqueous acidic medium. *Int. J. Electrochem. Sci.* **2020**, 3283–3297.

[15]. Hegazy, M. A.; Hasan, A. M.; Emara, M. M.; Bakr, M. F.; Youssef, A. H. Evaluating four synthesized Schiff bases as corrosion inhibitors on the carbon steel in 1 M hydrochloric acid. *Corros. Sci.* **2012**, *65*, 67–76.

[16]. Nathan, C. C. *Corrosion Inhibitors*; National Association of Corrosion Engineers (NACE), Houston: Texas, USA, 1973.

[17]. Gece, G. The use of quantum chemical methods in corrosion inhibitor studies. *Corros. Sci.* **2008**, *50*, 2981–2992.

[18]. El Adnani, Z.; Mcharfi, M.; Sfaira, M.; Benzakour, M.; Benjelloun, A. T.; Ebn Touhami, M. DFT theoretical study of 7-R-3methylquinoxalin-2(1H)-thiones (RH; CH3; Cl) as corrosion inhibitors in hydrochloric acid. *Corros. Sci.* **2013**, *68*, 223–230.

[19]. El-Naggar, M. M. Corrosion inhibition of mild steel in acidic medium by some sulfa drugs compounds. *Corros. Sci.* **2007**, *49*, 2226–2236.

[20]. Tüzün, B.; Bhawsar, J. Quantum chemical study of thiaozole derivatives as corrosion inhibitors based on density functional theory. *Arab. J. Chem.* **2021**, *14*, 102927.

[21]. Lee, C.; Yang, W.; Parr, R. G. Development of the Colle-Salvetti correlation-energy formula into a functional of the electron density. *Phys. Rev. B Condens. Matter* **1988**, *37*, 785–789.

[22]. Miehlich, B.; Savin, A.; Stoll, H.; Preuss, H. Results obtained with the correlation energy density functionals of becke and Lee, Yang and Parr. *Chem. Phys. Lett.* **1989**, *157*, 200–206.

[23]. Petersson, G. A.; Bennett, A.; Tensfeldt, T. G.; Al-Laham, M. A.; Shirley, W. A.; Mantzaris, J. A complete basis set model chemistry. I. The total energies of closed-shell atoms and hydrides of the first-row elements. *J. Chem. Phys.* **1988**, *89*, 2193–2218.

[24]. Sellaoui, L.; Guedidi, H.; Knani, S.; Reinert, L.; Duclaux, L.; Ben Lamine, A. Application of statistical physics formalism to the modeling of adsorption isotherms of ibuprofen on activated carbon. *Fluid Phase Equilib.* **2015**, *387*, 103–110.

[25]. Hassan, H. H.; Abdelghani, E.; Amin, M. A. Inhibition of mild steel corrosion in hydrochloric acid solution by triazole derivatives. *Electrochim. Acta* **2007**, *52*, 6359–6366.

[26]. Ramesh, S.; Rajeswari, S. Corrosion inhibition of mild steel in neutral aqueous solution by new triazole derivatives. *Electrochim. Acta* **2004**, *49*, 811–820.

[27]. Beda, R. H. B.; Niamien, P. M.; Avo Bilé, E. B.; Trokourey, A. Inhibition of aluminium corrosion in 1.0 M HCl by caffeine: Experimental and DFT studies. *Adv. Chem.* **2017**, *2017*, 1–10.

[28]. Khamaysa, O. M. A.; Selatnia, I.; Zeghache, H.; Lgaz, H.; Sid, A.; Chung, I.-M.; Benahmed, M.; Gherraf, N.; Mosset, P. Enhanced corrosion inhibition of carbon steel in HCl solution by a newly synthesized hydrazone derivative: Mechanism exploration from electrochemical, XPS, and computational studies. *J. Mol. Liq.* **2020**, *315*, 113805.

[29]. Karthikaiselvi, R.; Subhashini, S. Study of adsorption properties and inhibition of mild steel corrosion in hydrochloric acid media by water soluble composite poly (vinyl alcohol-omethoxy aniline). *J. Assoc. Arab Univ. Basic Appl. Sci.* **2014**, *16*, 74–82.

[30]. Chen, Y.; Chen, Z.; Zhuo, Y. Newly synthesized morpholinyl Mannich bases as corrosion inhibitors for N80 steel in acid environment. *Materials (Basel)* **2022**, *15*, 4218.

[31]. Tan, C. H. C.; Sabar, S.; Hussin, M. H. Development of immobilized microcrystalline cellulose as an effective adsorbent for methylene blue dye removal. *S. Afr. J. Chem. Eng.* **2018**, *26*, 11–24.

[32]. Akinbulumo, O. A.; Odejobi, O. J.; Odekanle, E. L. Thermodynamics and adsorption study of the corrosion inhibition of mild steel by Euphorbia heterophylla L. extract in 1.5 M HCl. *Results in Materials* **2020**, *5*, 100074.

[33]. Diki, N. Y. S.; Coulibaly, N. H.; Kassi, K. F.; Trokourey, A. Mild steel corrosion inhibition by synthesized 7-(Ethylthiobenzimidazolyl) Theophylline. *J. Electrochem. Sci. Eng.* **2021**, *11*, 97–106.

[34]. Abdul Rahiman, A. F. S.; Sethumanickam, S. Corrosion inhibition, adsorption and thermodynamic properties of poly(vinyl alcohol-cysteine) in molar HCl. *Arab. J. Chem.* **2017**, *10*, S3358–S3366.

[35]. Abdelshafi, N. S.; Sadik, M. A.; Shoeib, M. A.; Halim, S. A. Corrosion inhibition of aluminum in 1 M HCl by novel pyrimidine derivatives, EFM measurements, DFT calculations and MD simulation. *Arab. J. Chem.* **2022**, *15*, 103459.

[36]. Chen, L.; Lu, D.; Zhang, Y. Organic compounds as corrosion inhibitors for carbon steel in HCl solution: A comprehensive review. *Materials (Basel)* **2022**, *15*, 2023.

[37]. Merimi, I.; EL Ouadi, Y.; Benkaddour, R.; Lgaz, H.; Messali, M.; Jeffali, F.; Hammouti, B. Improving corrosion inhibition potentials using two triazole derivatives for mild steel in acidic medium: Experimental and theoretical studies. *Mater. Today* **2019**, *13*, 920–930.

[38]. Khadom, A. A.; Abd, A. N.; Ahmed, N. A. Xanthium strumarium leaves extracts as a friendly corrosion inhibitor of low carbon steel in hydrochloric acid: Kinetics and mathematical studies. *S. Afr. J. Chem. Eng.* **2018**, *25*, 13–21.

[39]. Ben Aoun, S. On the corrosion inhibition of carbon steel in 1 M HCl with a pyridinium-ionic liquid: chemical, thermodynamic, kinetic and electrochemical studies. *RSC Adv.* **2017**, *7*, 36688–36696.

[40]. Madkour, L. H.; Elshamy, I. H. Experimental and computational studies on the inhibition performances of benzimidazole and its derivatives for the corrosion of copper in nitric acid. *Int. J. Ind. Chem.* **2016**, *7*, 195–221.

[41]. Diki, N. Y. S.; Coulibaly, N. H.; Kambiré, O.; Trokourey, A. Experimental and theoretical investigations on copper corrosion inhibition by cefixime drug in 1M HNO3 solution. *J. Mater. Sci. Chem. Eng.* **2021**, *09*, 11–28.

[42]. Al-Amiery, A. A.; Mohamad, A. B.; Kadhum, A. A. H.; Shaker, L. M.; Isahak, W. N. R. W.; Takriff, M. S. Experimental and theoretical study on the corrosion inhibition of mild steel by nonanedioic acid derivative in hydrochloric acid solution. *Sci. Rep.* **2022**, *12*, 4705.

[43]. Li, X.; Deng, S.; Fu, H. Triazolyl blue tetrazolium bromide as a novel corrosion inhibitor for steel in HCl and H2SO4 solutions. *Corros. Sci.* **2011**, *53*, 302–309.

[44]. Faustin, M.; Maciuk, A.; Salvin, P.; Roos, C.; Lebrini, M. Corrosion inhibition of C38 steel by alkaloids extract of Geissospermum laeve in 1M hydrochloric acid: Electrochemical and phytochemical studies. *Corros. Sci.* **2015**, *92*, 287–300.

[45]. Deng, S.; Li, X. Inhibition by Jasminum nudiflorum Lindl. leaves extract of the corrosion of aluminium in HCl solution. *Corros. Sci.* **2012**, *64*, 253–262.